Springer

KSME

Journal of Mechanical Science and Technology 31 (1) (2017) 149~155
www.springerlink.com/content/1738-494x(Print)/1976-3824(Online)
DOI 10.1007/s12206-016-1214-2

Oxidation and thermal shock behavior of thermal barrier coated 18/10CrNi alloy with coating modifications †

Selim Gürgen[1,*], Seyid Fehmi Diltemiz[2] and Melih Cemal Kuşhan[3]

[1]*Vocational School of Transportation, Anadolu University, 26470, Eskişehir, Turkey*
[2]*Turkish Air Force, 1st Air Supply and Maintenance Center Command, 26320, Eskişehir, Turkey*
[3]*Department of Mechanical Engineering, Eskişehir Osmangazi University, 26480, Eskişehir, Turkey*

(Manuscript Received January 5, 2016; Revised July 27, 2016; Accepted August 1, 2016)

Abstract

In this study, substrates of 18/10CrNi alloy plates were initially sprayed with a Ni-21Cr-10Al-1Y bond coat and then with an yttria stabilized zirconia top coat by plasma spraying. Subsequently, plasma-sprayed Thermal barrier coatings (TBCs) were treated with two different modification methods, namely, vacuum heat treatment and laser glazing. The effects of modifications on the oxidation and thermal shock behavior of the coatings were evaluated. The effect of coat thickness on the bond strength of the coats was also investigated. Results showed enhancement of the oxidation resistance and thermal shock resistance of TBCs following modifications. Although vacuum heat treatment and laser glazing exhibited comparable results as per oxidation resistance, the former generated the best improvement in the thermal shock resistance of the TBCs. Bond strength also decreased as coat thickness increased.

Keywords: Laser glazing; Oxidation; Thermal barrier coating; Thermal shock; Vacuum heat treatment

1. Introduction

Thermal barrier coatings (TBCs) are used on blades and vanes of gas turbines to lower the surface temperature of base metals. TBCs also protect components from damages, such as oxidation, abrasion, and corrosion under service conditions [1]. Development of TBCs is significant for prolonging the lifetime of heat-resistant components.

TBC applications are performed through various techniques, such as air plasma spray, electron beam-physical vapor deposition, and high-velocity oxygen fuel. Modification methods can also be applied to the as-coated components for improving mechanical and thermal properties. TBCs exhibit a relatively short lifetime because of the thermal contrast between coating and base metal. Thermal residual stresses generated during the coating also deteriorate the thermal and mechanical properties of TBCs. Coating modifications enhance the strain tolerance of ceramic coats and reduce the residual stresses using various mechanisms [2, 3]. Vacuum heat treatment (VHT) and Laser glazing (LG) are preferable modification methods investigated in the literature. Previous studies [4-6] exhibited the improvement in the strength of bond coats and oxidation resistance using pre-oxidation methods including VHT. Park et al. [1] demonstrated the lengthened lifetime of plasma-sprayed TBCs after LG. Tsai et al. [7] and Lee et al. [8] revealed the improvement of microstructure and thermal cyclic performance of laser-glazed TBCs. Lee et al. [9] and Ding et al. [10] analyzed the residual stresses in plasma-sprayed TBCs, and they showed that residual stresses significantly affect the failure of TBCs. Damircheli et al. [11] investigated the influences of temperature and thickness on the thermal and mechanical stresses of functionally graded materials. Choi et al. [12] studied the effects of TBC thickness on bond strength and thermal fatigue behavior.

In this study, we focused on the oxidation and thermal shock resistance of TBCs after two different modification methods, namely, VHT and LG. The effects of these methods were evaluated by comparing the results with those of the as-coated TBCs without any modifications. During experiment, substrates of 18/10CrNi alloy plates were initially sprayed with a Ni-21Cr-10Al-1Y bond coat and then with an Yttria stabilized zirconia (YSZ) top coat by plasma spraying. Subsequently, plasma-sprayed TBCs were treated with VHT and LG. The effect of coat thickness on the bond strength of the coats was also investigated. The results showed enhancement of the oxidation resistance and thermal shock resistance of TBCs after the modifications. Although VHT and LG achieved comparable results in oxidation resistance results, the former provided the best improvement in thermal shock resis-

*Corresponding author. Tel.: +90 222 224 13 91, Fax.: +90 222 224 13 92
E-mail address: selimgurgen@anadolu.edu.tr
† Recommended by Associate Editor Nam-Su Huh

Table 1. Properties of coating powders.

Powder	Coating type	Particle size range (μm)	Chemical composition (wt%)
Amdry 962	Bond coat	−106+52	Ni-21Cr-10Al-1Y
Metco 204NS	Top coat	−106+11	ZrO_2-8Y_2O_3

Table 2. Processing parameters of plasma spray for coating operations.

	Coating condition	
Parameters	Bond coating	Top coating
Primary plasma gas, pressure and flow rate (mbar-l/min)	Ar 690-37.8	Ar 690-37.8
Secondary plasma gas, pressure and flow rate (mbar-l/min)	H_2 345-7.1	H_2 345-7.1
Powder carrier gas, pressure and flow rate (mbar-l/min)	Ar 345-8.3	Ar 345-8.3
Powder feed rate (g/min)	30	40
Torch to specimen distance (mm)	115	115
Number of pass	2	3
Current (A)	500	450
Voltage (V)	60	60

tance of the TBCs. Bond strength also decreased as coat thickness increased.

2. Materials and method

In this study, 18/10CrNi plates were used as the base material for the coatings. Three different specimen sizes were employed (30×25×4 mm^3 for thermal shock, 25×25×4 mm^3 for oxidation, and Ø25×4 mm^3 for bond strength tests). Before coating, specimens were grit-blasted to prepare the substrate surfaces. Bond coat was deposited using a nickel-based powder onto specimens. Powders with hollow sphere particles were selected for the top coating. Table 1 lists the properties of the powders used in coating.

Coating operations were performed using a 9 MB plasma spray gun (Sulzer Metco) modified with the ABB robotic system to enhance its precision. Table 2 provides the process parameters for bond and top coating operations.

After coating, a set of specimens was kept as As-coated (AC) samples and two modification methods were applied to the remaining coated specimens. The first method, VHT, was a type of pre-oxidation method. For this treatment, specimens were placed in an industrial vacuum furnace at 1080 °C for 30 min. The second modification method, LG, was carried out with a Nd:YAG laser (Huffman HP-8S8). To obtain the optimum process parameters for LG, a coated disk with a diameter of 100 mm was laser glazed with various parameters (Fig. 1). After the microstructural investigation of the sample disk, parameters for LG were selected (Table 3).

3. Experimental details

In the experimental stage of the study, bond strength, oxidation resistance, and thermal shock resistance of the TBCs were investigated. In the microstructural analyses, images were obtained using optical microscopy with Nikon Optiphot-100 and scanning electron microscopy with Leo-S440. In the post-processing stage, NIS-elements and Leica image analyzer software programs were used to calculate the areal percentage of Thermally grown oxide (TGO) in the cross-sectional area of the specimens. One cross-sectional view was insufficient to reveal the true results because TGO formation occurred at the dendritic and rough interfaces between the coats. The results were evaluated using 20 cross-sectional views along each specimen, thereby achieving a good distribution that considered various regions in the specimens. Prior to the microstructural analyses, specimens were prepared with a metallographic sample preparation procedure, as listed in Table 4. The sectioning step was performed using a Struers Secotom-10 cut-off machine at a reduced cutting speed to minimize plastic deformation and heat generation. Grinding steps were completed with a Buehler Phoenix-4000 sample preparation system. Prior to grinding, specimens were vacuum cold molded with epoxy resin.

Table 3. Processing parameters for LG.

Parameters	
Average laser power	240 W
Wavelength	1.06 μm
Spot size	4.1 mm
Track shift	2 mm
Scanning speed	120 mm/min
Pulse frequency	30 Hz

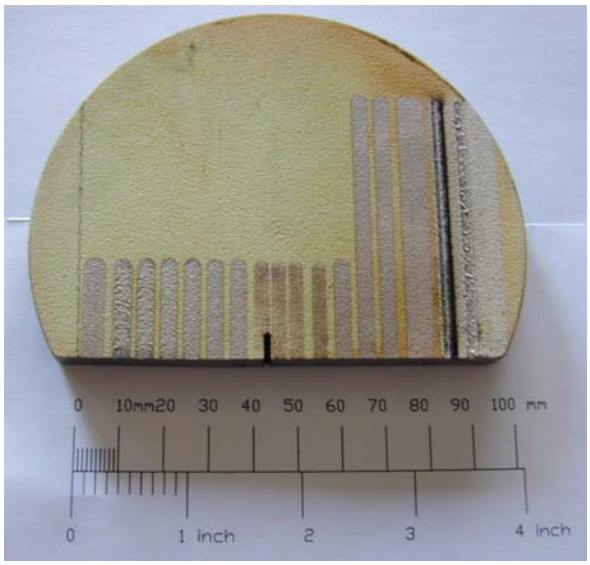

Fig. 1. Laser-glazed sample disk after various operations.

3.1 Bond strength testing

To test bond strength, the effect of top coat thickness was

Table 4. Metallographic sample preparation procedure.

Step	Operation	Material	Load (N)	Time (min)
1	Sectioning	Al_2O_3 disk	-	-
2	Cold molding	Epoxy resin	-	480
3	Grinding	SiC-220 grit	18	2
4	Grinding	SiC-320 grit	18	1
5	Grinding	SiC-500 grit	18	1
6	Grinding	SiC-800 grit	18	1
7	Grinding	SiC-1200 grit	18	1
8	Grinding	Diamond-3 μm particle	22	6
9	Grinding	Diamond-1 μm particle	20	3

investigated using AC specimens with different top coat thicknesses. Thickness variation was achieved by changing the number of gun passes during coating. The bond strength of the coatings were tested according to GE:E50TF60 [13]. Each coated specimen was placed between two axially symmetric rods, and the interfaces between the specimen and the rods were affixed using an epoxy-based structural adhesive (EC-2086, 3M). Specimens were then compressed on a fixture and cured in an industrial furnace at 185 °C for 2 h. After curing, specimens were cooled to room temperature in the furnace, and the rods were connected to a servo-hydraulic Instron 5985 testing machine for tensile testing performed with a constant crosshead speed of 2 mm/min. Tests were pursued until failure of the specimens and strength of the coatings were calculated with the load of failure per specimen area.

3.2 Oxidation testing

Oxidation resistance of the specimens was tested using the regular method for coated jet engine components. To expedite the testing, specimens were subjected to conditions more crucial than service conditions. Each specimen was placed in an industrial furnace at 1120 °C for 23 h and cooled to room temperature in the furnace. During evaluation, the interfaces between base metal/bond coat and bond coat/top coat were investigated using micrographs. The average thickness of the coats was measured according to ASTM B487 [14]. In addition, four specimens with only bond coats were tested at 1120 °C at various durations. The four specimens were removed from the furnace after 8, 24, 48 and 64 h to determine the percentage of oxidation with respect to oxidation time.

3.3 Thermal shock testing

Thermal shock testing was performed with a computer-controlled system. Specimens were placed between two ceramic grips, and coated surfaces were subjected to cyclic oxy-acetylene flame (Fig. 2). Each cycle lasted 60 s, that is, 30 s with activated flame and the subsequent 30 s with deactivated flame. The measurements showed that the maximum temperature at the back surface of the specimens varied from 550 °C to 900 °C for each thermal cycle. Specimens were cooled to room temperature after 50 cycles, and tests were terminated after 350 cycles.

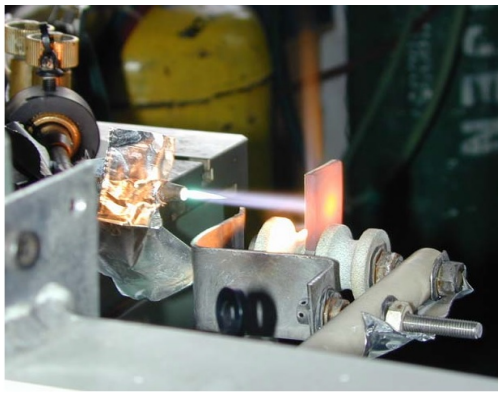

Fig. 2. A specimen during thermal cycle.

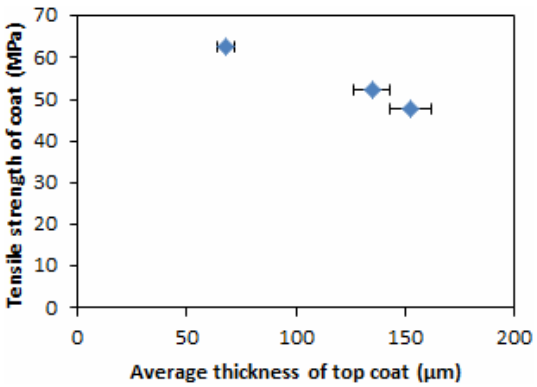

Fig. 3. Tensile strength vs. average thickness of top coat.

4. Results and discussion

4.1 Bond strength of the coatings

Fig. 3 shows tensile strength of the coats versus thickness of the top coats. Tensile strength changes inversely with coat thickness. This finding is explained by the residual stress perpendicular to the top coat, which increases as the thickness of coat increases [12, 15]. Choi et al. [12] verified this relation using finite element simulations and x-ray diffraction method. Notably, thin coats are slightly affected by non-axial loads during the tensile testing. Failure in the specimens is located at the top coats and interface of the bond and top coats. These findings indicate that bond coats are superior in strength than top coats. Metallic coatings onto metals (e.g., the bond coating in this study), are intensely strong [16]. Lima et al. [16] stated that metallic bond coatings on metal substrates significantly increase in bond strength with respect to ceramic coatings. Furthermore, the strength of the bond coat can be explained by a mechanically interlocking mechanism, which is defined as anchorage of the feedstock droplets to the irregularities on the

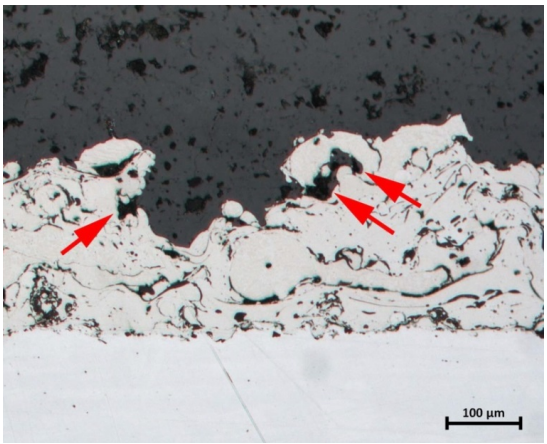

Fig. 4. Voids at the interface of bond and top coats in AC specimen.

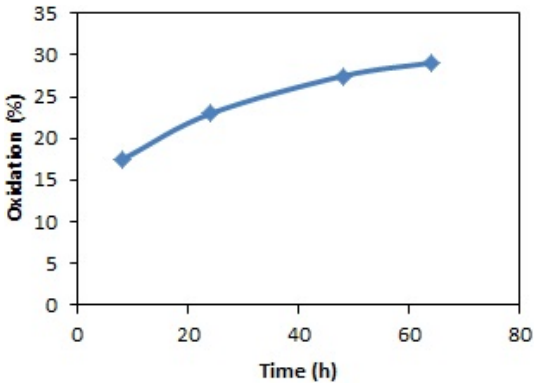

Fig. 5. Oxidation percentage vs. time in bond coated specimens.

substrate. Such irregularities are formed with any surface preparation method, such as grit-blasting, prior to coating [17]. After the solidification of the feedstock droplets, they shrink around the irregularities and adhere to the substrate with a strong force [18]. However, the surface of the bond coat that forms the interface of bond and top coats may include excessive irregularities, such as crooked overhangs. These regions are inaccessible cavities for the droplets of the top coat feedstock. Therefore, the strength of the bond coat/top coat interface reduces because of the increased number of voids formed during coating. Fig. 4 shows the voids at the bond coat/top coat interface.

4.2 Oxidation resistance of the coatings

Fig. 5 shows the oxidation characteristics of the bond coated specimens with respect to the oxidation time. The graph clearly presents that oxidation in the bond coat increases degressively with time. At the beginning of the oxidation test, TGO formation rapidly occurs in the specimen. At the latter stages, TGO formation decelerates because of the oxide layers blocking the oxygen transfer into the specimen [19, 20]. During thermal exposure, TGO layers preferentially include alumina, which ensures good diffusion barrier for the coats [20, 21]. Oxides of Cr/Ni/Co, which represent a cluster of mixed formations, may be observed in the TGO layers. Such cluster groups are called spinels and found to be the preferred sites of crack nucleation in the coatings [22]. These detrimental oxides generate vertical stresses owing to the rapid local volume increase at the interface of the TGO and coats [22-24]. However, dense and continuous TGO layers of alumina hinder the formation of detrimental oxides during thermal exposure [5, 25, 26]. Alumina layers also exhibit higher fracture toughness than the spinel groups [24]. To identify the oxide layers in the specimens, AC and VHT specimens were investigated using energy dispersive spectroscopy. Measurements were performed with several spot analyses on the oxide layers. Aluminum content in the TGO layers increases after VHT because the average aluminum concentration is 20.46 % and 24.07 % for AC and VHT specimens, respectively. This result suggests that VHT suppresses the formation of detrimental oxides by developing alumina layers. VHT enriches the preferred alumina formation in the oxide layers, and this outcome is consistent with the results from previous experiments [5, 6, 25-28].

Table 5 provides the average areal percentage of TGO in the bond coat of the specimens before and after the oxidation tests. The graph indicates that final oxide percentage is higher in AC specimens than in other specimens. The lowest percentage is found in LG specimens. To consider the initial oxide percentage, the Oxidation growth rate (OGR %) is defined in Eq. (1).

$$OGR\% = \frac{Final\ oxide\% - Initial\ oxide\%}{Final\ oxide\%}. \quad (1)$$

Based on the OGR% results, AC specimens exhibit quicker response to the oxidation affinity in the bond coat than other specimens do. VHT and LG specimens are less prone to oxidation, although they achieved comparable results. Both VHT and LG positively influence oxidation resistance of the coated specimens. VHT contributes to the development of an oxide layer during pre-oxidation that acts as a barrier for oxygen penetration, thereby increasing oxidation resistance with respect to the AC specimen [19, 20]. On the contrary, oxidation resistance in LG specimens is explained by the remelted layer on the surface of the top coat. After LG, the remelted layer provides a continuous and non-porous surface segment at the top coat, thereby hindering the penetration of oxygen into the coating [1, 7]. The segmented surface morphology is formed owing to the vertical cracks connected to each other with a net-shaped formation on the surface (Fig. 6). These cracks are formed during cooling after LG, and the crack sizes increase as the laser power increases. Unlike in the non-porous surface, vertical cracks allow oxygen infiltration to the lower coating layers, but the overall protection against the infiltration is increased; therefore, oxidation resistance of the coating is improved after LG [1].

Table 5. Percentage of TGO.

Measurement	Specimen		
	AC	VHT	LG
Initial oxidation	12.80 %	14.15 %	12.76 %
Final oxidation	34.66 %	33.14 %	30.68 %
OGR%	63.07 %	57.30 %	58.41 %

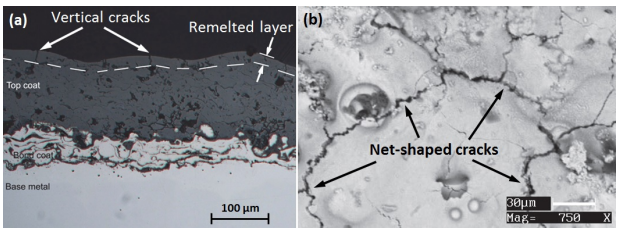

Fig. 6. (a) Cross-sectional; (b) surface view of LG specimen.

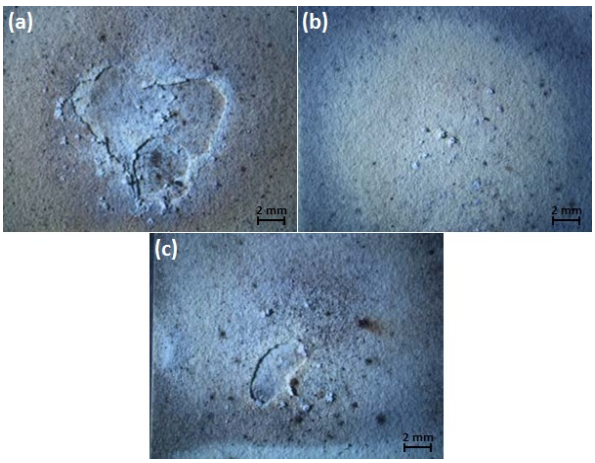

Fig. 7. Surface of (a) AC; (b) VHT; (c) LG after thermal shock test.

4.3 Thermal shock resistance of the coatings

Fig. 7 shows the damaged area of each specimen after thermal shock testing. Clearly, thermal shock is more destructive for AC specimens than other specimens. LG enhances the thermal shock resistance, but VHT provides the best thermal shock resistance for the specimens because no visible delamination or cracking is observed on the surface following vacuum heat application. Under cyclic thermal exposure, base metal and coats exhibit different expansion and shrinkage responses caused by the different coefficients of thermal expansion. Consequently, this contradiction creates the mismatch between the base metal and the top coat, thereby accelerating the evolution of microcracks in the ceramic top coat. Thermal residual stresses are also generated in the structure during TBC. Accumulation of thermal residual stresses stimulates the propagation of microcracks in the ceramic coat; therefore, the AC specimens exhibit a relatively short lifetime under loading conditions [3]. However, following a stress relief operation such as VHT, the residual stresses are eliminated and the structure improves the mechanical properties,

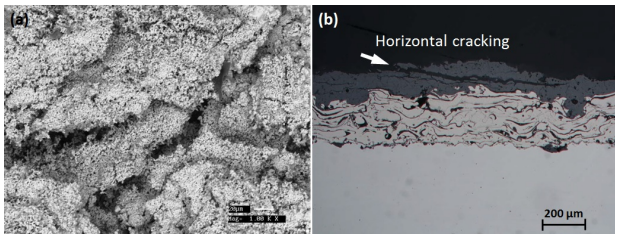

Fig. 8. (a) Maximum damaged point on AC specimen surface; (b) horizontal cracking inside the top coat.

thus explaining the improved thermal shock resistance of VHT specimens. Apart from the failure mechanism under cyclic thermal loading, YSZ is generally preferable for the top coating to eliminate the divergence in the thermal expansion of the base metal and ceramic coat because its high coefficient of thermal expansion closely matches that of the base metal [29]. Nevertheless, YSZ is not an exact solution for the removal of said effect in the structure. The thermal shock resistance of LG specimens improves through the presence of net-shaped cracks. Stresses during the thermal cycle do not directly accumulate into the coating in the macro scale because the net-shaped cracks provide stress relief for the segmented structure and increase the strain tolerance of the top coat [30]. Young's modulus of the top coat also lessens as the density of the vertical cracks increases [31]. The mismatch of thermal stress between the base metal and the top coat is reduced [7, 8]. Consequently, LG increases the thermal shock resistance of TBCs by forming vertical cracks in the top coat.

Fig. 8(a) shows the maximum damaged point on the surface of AC specimens. The maximum damage is located at the central point of the surface, which is directly subjected to the flame during the thermal shock testing. Within this vicinity, the top coat layers are partially melted and sintered because of excessive thermal exposure. Thus, sintering enhances the strain accumulation in the top coat and induces horizontal cracking within the top coat and at the interface of the bond coat/top coat (Fig. 8(b)). At the latter stages, these cracks reach the free surfaces and pull out the layers from the coat in the form of flakes [18, 32]. This type of delamination arises from the thermal stresses without mechanical loadings on the coated surfaces.

5. Conclusion

This study investigated the effects of VHT and LG on TBCs deposited on 18/10CrNi alloy plates by plasma spraying. Influences were evaluated in terms of oxidation and thermal shock resistance of the modified coatings in comparison with the AC specimens. The effect of coat thickness on the bond strength of the coats was also investigated. The results indicate that VHT causes pre-oxidation inside the coats, thereby hindering the diffusion of oxygen into the lower layers of the coat and increasing the oxidation resistance in the structure. Conversely, LG forms remelted surface layers on the top coat and

provides non-porous and segmented morphology for the surface. Oxygen penetration is prevented and oxidation resistance is increased in the VHT and LG specimens compared with the AC specimens in which even the vertical cracks on the surface allow the oxygen transfer into the coats. Regarding thermal shock resistance, VHT provides stress relief for TBCs. Vertical cracks due to the cooling period following LG generate the stress relief regions in the structure, thereby enhancing thermal shock resistance. Notably, bond strength of the coats inversely changes with coat thickness.

Acknowledgements

The authors gratefully acknowledge the facilities provided by the Turkish Air Force, 1st Air Supply and Maintenance Center Command. S. Gürgen also acknowledges the support of the Scientific and Technological Research Council of Turkey under Program 2211.

References

[1] J. H. Park, J. S. Kim, K. H. Lee, Y. S. Song and M. C. Kang, Effects of the laser treatment and thermal oxidation behavior of CoNiCrAlY/ZrO2-8wt%Y2O3 thermal barrier coating, *J. Mater. Process. Technol.*, 201 (1-3) (2008) 331-335.

[2] B. S. Yilbas, A. F. M. Arif and M. A. Gondal, HVOF coating and laser treatment: three-point bending tests, *J. Mater. Process. Technol.*, 164-165 (2005) 954-957.

[3] R. Ahmadi-Pidani, R. Shoja-Razavi, R. Mozafarinia and H. Jamali, Improving the thermal shock resistance of plasma sprayed CYSZ thermal barrier coatings by laser surface modification, *Opt. Lasers Eng*., 50 (5) (2012) 780-786.

[4] B. Gorr, S. Burk, V. B. Trindade and H.-J. Christ, The effect of pre-oxidation treatment on the high-temperature oxidation of Co-Re-Cr model alloys at laboratory air, *Oxid. Met.*, 74 (5-6) (2010) 239-253.

[5] W. R. Chen, X. Wu, B. R. Marple, R. S. Lima and P. C. Patnaik, Pre-oxidation and TGO growth behaviour of an air-plasma-sprayed thermal barrier coating, *Surf. Coat. Technol.*, 202 (16) (2008) 3787-3796.

[6] W. R. Chen, R. Archer, X. Huang and B. R. Marple, TGO Growth and Crack Propagation in a Thermal Barrier Coating, *J. Therm. Spray Technol*., 17 (5-6) (2008) 858-864.

[7] H. Tsai and P. Tsai, Microstructures and Properties of Laser-Glazed Plasma-Sprayed ZrO2-YO1.5/Ni-22Cr-10AI-1Y Thermal Barrier Coatings, *J. Mater. Eng. Perform.,* 4 (6) (1995) 689-696.

[8] J.-H. Lee, P.-C. Tsai and C.-L. Chang, Microstructure and thermal cyclic performance of laser-glazed plasma-sprayed ceria-yttria-stabilized zirconia thermal barrier coatings, *Surf. Coat. Technol.*, 202 (22-23) (2008) 5607-5612.

[9] M.-J. Lee, B.-C. Lee, J.-G. Lim and M.-K. Kim, Residual stress analysis of the thermal barrier coating system by considering the plasma spraying process, *J. Mech. Sci. Technol*., 28 (6) (2014) 2161-2168.

[10] J. Ding, F.-X. Li and K.-J. Kang, Numerical simulation of displacement instabilities of surface grooves on an alumina forming alloy during thermal cycling oxidation, *J. Mech. Sci. Technol.*, 23 (8) (2009) 2308-2319.

[11] M. Damircheli and M. Azadi, Temperature and thickness effects on thermal and mechanical stresses of rotating FG-disks, *J. Mech. Sci. Technol.*, 25 (3) (2011) 827-836.

[12] H. M. Choi, B. S. Kang, W. K. Choi, D. G. Choi, S. K. Choi, J. C. Kim, Y. K. Park and G. M. Kim, Effect of the thickness of plasma-sprayed coating on bond strength and thermal fatigue characteristics, *J. Mater. Sci.*, 33 (1998) 5895-5899.

[13] GE: E50TF60, *Bond Strength of Thermal Sprayed Coatings,* General Electric, USA (1993).

[14] ASTM B487, *Standard Test Method for Measurement of Metal and Oxide Coating Thickness by Microscopical Examination of Cross Section*, ASTM International, West Conshohocken, USA (2013).

[15] S. Bose, *High temperature coatings,* Elsevier Butterworth-Heinemann, Boston, USA (2007).

[16] C. R. C. Lima and R.-E. Trevisan, Graded plasma spraying of premixed metalceramic powders on metallic substrates, *J. Therm. Spray Technol.*, 6 (2) (1997) 199-204.

[17] A. M. Limarga, S. Widjaja and T. H. Yip, Mechanical properties and oxidation resistance of plasma-sprayed multilayered Al2O3/ZrO2 thermal barrier coatings, *Surf. Coat. Technol.*, 197 (1) (2005) 93-102.

[18] R. B. Heimann, *Plasma-spray coating principles and applications*, VCH Publishers, New York, USA (1996).

[19] A. M. Limarga, R. Vaßen and D. R. Clarke, Stress distributions in plasma-sprayed thermal barrier coatings under thermal cycling in a temperature gradient, *J. Appl. Mech.*, 78 (1) (2011) 0110031-0110039.

[20] M. Daroonparvar, M. Azizi Mat Yajid, N. M. Yusof and M. Sakhawat Hussain, Improved Thermally Grown Oxide Scale in Air Plasma Sprayed NiCrAlY/Nano-YSZ Coatings, *J. Nanomater.*, 2013 (2013) 1-9.

[21] M. Daroonparvar, M. S. Hussain and M. A. M. Yajid, The role of formation of continues thermally grown oxide layer on the nanostructured NiCrAlY bond coat during thermal exposure in air, *Appl. Surf. Sci.*, 261 (2012) 287-297.

[22] A. Rabiei, Failure mechanisms associated with the thermally grown oxide in plasma-sprayed thermal barrier coatings, *Acta Mater.*, 48 (15) (2000) 3963-3976.

[23] W. R. Chen, X. Wu, D. Dudzinski and P. C. Patnaik, Modification of oxide layer in plasma-sprayed thermal barrier coatings, *Surf. Coat. Technol.*, 200 (20-21) (2006) 5863-5868.

[24] A. G. Evans, D. R. Mumm, J. W. Hutchinson, G. H. Meier and F. S. Pettit, Mechanisms controlling the durability of thermal barrier coatings, *Prog. Mater. Sci.*, 46 (5) (2001) 505-553.

[25] T. J. Nijdam, L. P. H. Jeurgens, J. H. Chen and W. G. Sloof, On the microstructure of the initial oxide grown by controlled annealing and oxidation on a NiCoCrAlY bond coating, *Oxid. Met.*, 64 (5-6) (2005) 355-377.

[26] T. J. Nijdam, G. H. Marijnissen, E. Vergeldt, A. B. Kloosterman and W. G. Sloof, Development of a pre-

oxidation treatment to improve the adhesion between thermal barrier coatings and NiCoCrAlY bond coatings, *Oxid. Met.*, 66 (5-6) (2006) 269-294.

[27] W. R. Chen, X. Wu, B. R. Marple, D. R. Nagy and P. C. Patnaik, TGO growth behaviour in TBCs with APS and HVOF bond coats, *Surf. Coat. Technol.*, 202 (12) (2008) 2677-2683.

[28] V. K. Tolpygo and D. R. Clarke, The effect of oxidation pretreatment on the cyclic life of EB-PVD thermal barrier coatings with platinum-aluminide bond coats, S*urf. Coat. Technol.*, 200 (5-6) (2005) 1276-1281.

[29] M. Saremi, A. Afrasiabi and A. Kobayashi, Microstructural analysis of YSZ and YSZ/Al2O3 plasma sprayed thermal barrier coatings after high temperature oxidation, *Surf. Coat. Technol.,* 202 (14) (2008) 3233-3238.

[30] S. Ahmaniemi, P. Vuoristo, T. Mäntylä, C. Gualco, A. Bonadei and R. Di Maggio, Thermal cycling resistance of modified thick thermal barrier coatings, *Surf. Coat. Technol*., 190 (2-3) (2005) 378-387.

[31] D. Schwingel, R. Taylor, T. Haubold, J. Wigren and C. Gualco, Mechanical and thermophysical properties of thick PYSZ thermal barrier coatings: correlation with microstructure and spraying parameters, *Surf. Coat. Technol*., 108-109 (1998) 99-106.

[32] M. Bartsch, B. Baufeld, S. Dalkilic, L. Chernova and M. Heinzelmann, Fatigue cracks in a thermal barrier coating system on a superalloy in multiaxial thermomechanical testing, *Int. J. Fatigue*, 30 (2) (2008) 211-218.

Selim Gürgen is a Research Assistant in Vocational School of Transportation, Anadolu University. He worked as a Manufacturing Engineer in aerospace industry for three years. He contributed to several industrial and research projects on materials science and manufacturing.

Seyid Fehmi Diltemiz received his B.Sc. from Yıldız Technical University and Ph.D. from Eskişehir Osmangazi University. He has been working as a Metallurgical Specialist in Turkish Air Force, 1st Air Supply and Maintenance Center Command for eleven years. He deals with thermal barrier coating and failure analysis in jet engines.

Melih Cemal Kuşhan is an Associate Professor of Mechanical Engineering in Eskişehir Osmangazi University. He is the author or co-author of more than 25 scientific articles and 50 conference papers. He has also a book and three book chapters in international books about aviation. His research area is materials science.